

Symmetry Improved 2PI Effective Action and the Infrared Divergences of the Standard Model

Apostolos Pilaftsis, Daniele Teresi

Consortium for Fundamental Physics, School of Physics and Astronomy,
University of Manchester, Manchester M13 9PL, United Kingdom.

E-mail: Apostolos.Pilaftsis@manchester.ac.uk, Daniele.Teresi@manchester.ac.uk

Abstract. Resummations of infinite sets of higher-order perturbative contributions are often needed both in thermal field theory and at zero temperature. For instance, the behaviour of the Standard Model (SM) effective potential extrapolated to very high energies is known to be extremely sensitive to higher-order effects. The 2PI effective action provides a systematic approach to consistently perform such resummations. However, one of its major limitations was that its loopwise expansion introduces residual violations of possible global symmetries, thus giving rise to massive Goldstone bosons in the spontaneously broken phase of the theory. We review the recently developed symmetry-improved 2PI formalism for consistently encoding global symmetries in the 2PI approach, and discuss its satisfactory field-theoretical properties. We then apply the formalism to study the infrared divergences of the SM effective potential due to Goldstone bosons, which may affect the stability analyses of the SM. We present quantitative comparisons, for the scalar sector of the SM, with the approximate partial resummation procedure recently developed to address this problem, and show the quantitative discrepancy of the latter with the more complete 2PI approach, thus motivating further studies in this direction.

1. Introduction

In thermal field theory, finite-order perturbative expansions break down at high temperatures and one needs to resum higher-order contributions to deal with this problem. On the other hand, also at zero temperature there are situations where higher-order effects may potentially play an important role, even in a small-coupling regime. For instance, it has recently become well known that the behaviour of the Standard Model (SM) effective potential, extrapolated to very high energies, is extremely sensitive to the physics at the electroweak scale [1, 2, 3]. Thus, a formalism to incorporate and resum higher-order effects in a consistent manner is highly desirable for of both thermal and non-thermal applications.

A natural framework to address such problems is the formalism introduced by Cornwall, Jackiw and Tomboulis (CJT) [4]. Its simplest version is known as the Two-Particle-Irreducible (2PI) effective action. This is an effective action expressed not only in terms of the field, but also in terms of dressed propagators. When one considers a given truncation to the 2PI effective action, at any given order of the loopwise expansion, the 2PI effective action resums, automatically, an infinite set of higher-order diagrams induced by partially resummed propagators, without the danger of over-counting graphs.

So far, the 2PI formalism has been mainly used in thermal contexts, both at equilibrium [5, 6, 7, 8, 9] and out of equilibrium [10, 11, 12, 13]. One of the major limitations for its application to

zero-temperature problems like, for example, the study of the SM effective potential, has been the well-known difficulties of the CJT formalism to incorporate symmetries in a satisfactory way. In particular, global symmetries are not exactly maintained at a given loop order of the 2PI expansion, since they get distorted by higher-order effects, and this results in violation of the Goldstone theorem [14, 15] by higher-order terms, giving rise to a massive Goldstone boson in the Spontaneous Symmetry Breaking (SSB) phase of the theory [16, 17, 18, 19]. In the past, several studies were presented in the literature, attempting to provide a satisfactory solution to this problem (see references in [20]).

We have recently developed a new *symmetry-improved CJT formalism* [20] that addresses this long-standing problem and allows one to consistently use the 2PI effective action to study theories with global symmetries. In the symmetry-improved 2PI formalism, the Ward Identities (WIs) associated with global symmetries provide additional constraints for the extremal solutions of the fields and propagators. This formalism has a number of satisfactory field-theoretical properties, and actually provides an improvement over the standard CJT formulation, in the sense that the behaviour expected for the full theory is recovered already at a low orders of approximation. The symmetry-improved formalism has been also used to study the chiral phase transition [21], and it has recently been extended to higher n PI effective actions [22], confirming its consistency also when one goes beyond the 2PI approach.

It has been recently pointed out [23] that the SM effective potential suffers from infrared (IR) divergences due to the Goldstone bosons of the electroweak gauge group, which appear at three-loop order. They appear at two loops for the derivative of the potential, i.e. for the minimization condition that fixes the value of the Higgs vacuum expectation value (VEV). This problem needs to be addressed for a two-fold reason. From the conceptual point of view, the effective potential should be well-defined for all values of the Higgs background field ϕ . On the other hand, from the quantitative point of view, the appearance of these IR divergences formally lowers the order of the involved three- and higher-loop contributions, thus breaking down perturbation theory and potentially giving a significant contribution to the threshold corrections to the VEV. Because of the extreme sensitivity of the effective potential extrapolated at high energies to the matching conditions at the electroweak scale, this could result on quantitative sizable effects on the stability analyses of the SM potential. These issues have been recently addressed by means of an approximate partial resummation procedure, developed in [24, 25]. In addition to confirming the disappearance of the IR divergences within our approach, we will show that the more complete 2PI analysis, based on our symmetry-improved formalism, gives quantitatively different results, at least for the scalar sector of the SM. This suggests that even for the full SM there might be quantitative discrepancies between the approximate resummation scheme of [24, 25] and the 2PI approach, thus motivating further studies in this direction [26].

The layout of the paper is as follows. In Sections 2 and 3 we review the standard and symmetry-improved 2PI formalisms, respectively. In Section 4 we consider the first non-trivial truncation of the effective action, known as the Hartree-Fock (HF) approximation, for a scalar $\mathbb{O}(2)$ model, and demonstrate some of the satisfactory field-theoretical properties of the formalism. In Section 5 we go beyond this approximation and show that the symmetry-improved approach describes correctly the thresholds of the Higgs and Goldstone self-energies, in agreement with unitarity requirements. Moreover, we demonstrate explicitly how the formalism implicitly resums sets of processes at arbitrarily high order. Finally, in Section 6 we use the symmetry-improved 2PI effective action to study the issue of IR divergences in a global $SU(2) \times U(1)$ scalar model. We draw our conclusions in Section 7.

2. CJT Effective Action

In this section we briefly review the CJT formalisms. For concreteness, we consider a $\mathbb{O}(N)$ scalar model and show that, as opposed to the 1PI formalism, loopwise truncations of the

CJT generating effective action lead to violation of the Goldstone theorem through higher-order terms.

The model under consideration here is the $\mathbb{O}(N)$ scalar model described by the Lagrangian

$$\mathcal{L}[\phi] = \frac{1}{2} (\partial_\mu \phi^i) (\partial^\mu \phi^i) + \frac{m^2}{2} (\phi^i)^2 - \frac{\lambda}{4} (\phi^i)^2 (\phi^j)^2, \quad (2.1)$$

where $\phi^i = (\phi^1, \phi^2, \dots, \phi^N)$ represents the $\mathbb{O}(N)$ scalar multiplet and summation over the repeated indices $i, j = 1, 2, \dots, N$ is implied. At zero temperature, $T = 0$, the model has a SSB phase for $m^2 > 0$, with breaking pattern: $\mathbb{O}(N) \rightarrow \mathbb{O}(N-1)$. As a consequence of the Goldstone theorem [14, 15], there are $N-1$ Goldstone bosons and one Higgs particle H . For the simple case $N = 2$, which we are considering here, the field components $\phi^{1,2}$ may be decomposed as

$$\phi^H \equiv \phi^1 = \langle \widehat{\phi}^1 \rangle + H, \quad \phi^G \equiv \phi^2 = G, \quad (2.2)$$

where we have denoted field operators with a caret. Here, G is the Goldstone field, which is massless at the minimum of the potential, whereas H is the Higgs boson, which is in general massive.

The CJT effective action is the generalization of the 1PI one, where in addition to the local source J_x , multi-local sources are introduced. In its simplest version, the 2PI formalism, we consider one local and one bi-local source, i.e. J_x and K_{xy} . Therefore, the connected generating functional $W[J, K]$ is given by

$$W[J, K] = -i \ln \int \mathcal{D}\phi^i \exp \left[i \left(S[\phi] + J_x^i \phi_x^i + \frac{1}{2} K_{xy}^{ij} \phi_x^i \phi_y^j \right) \right], \quad (2.3)$$

where $S[\phi] = \int_x \mathcal{L}[\phi]$ is the classical action. Here and in the following, repeated spacetime coordinates will denote integration with respect to these coordinates. The background fields ϕ_x^i and the connected propagator Δ_{xy}^{ij} are obtained by single and double functional differentiation of $W[J, K]$ with respect to the source J_x^i :

$$\frac{\delta W[J, K]}{\delta J_x^i} \equiv \phi_x^i, \quad -i \frac{\delta W[J, K]}{\delta J_x^i \delta J_y^j} = \langle \widehat{\phi}_x^i \widehat{\phi}_y^j \rangle - \langle \widehat{\phi}_x^i \rangle \langle \widehat{\phi}_y^j \rangle \equiv i \Delta_{xy}^{ij}. \quad (2.4)$$

We also have

$$\frac{\delta W[J, K]}{\delta K_{xy}^{ij}} = \frac{1}{2} \left(i \Delta_{xy}^{ij} + \phi_x^i \phi_y^j \right). \quad (2.5)$$

The 2PI effective action $\Gamma[\phi, \Delta]$ is obtained as the double Legendre transform of $W[J, K]$ with respect to J and K :

$$\Gamma[\phi, \Delta] = W[J, K] - J_x^i \phi_x^i - \frac{1}{2} K_{xy}^{ij} \left(i \Delta_{xy}^{ij} + \phi_x^i \phi_y^j \right). \quad (2.6)$$

This has the explicit form [4]:

$$\Gamma[\phi, \Delta] = S[\phi] - \frac{i}{2} \text{Tr} \left(\ln \Delta \right) + \frac{i}{2} \text{Tr} \left(\Delta^{(0)-1} \Delta \right) - i \Gamma^{(\geq 2)}, \quad (2.7)$$

where $\Delta_{xy}^{(0)-1, ij} = \delta^2 S[\phi] / (\delta \phi_x^i \delta \phi_y^j)$ is the inverse tree-level propagator matrix and $\Gamma^{(\geq 2)}$ is the diagrammatic series of all two- and higher-loop 2PI vacuum diagrams in which the dressed

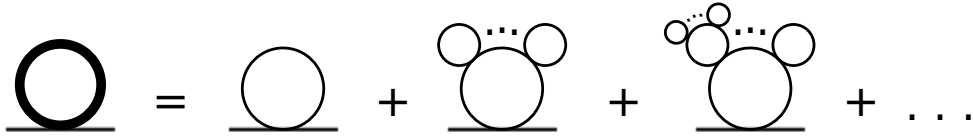


Figure 1. Infinite set of perturbation-theory diagrams implicitly resummed, in the 2PI formalism, by the self-energy on the LHS. Thick lines represent the full propagator, thin lines the tree-level one.

propagator matrix Δ is used, instead of the tree-level one. The equations of motions (EoMs) are obtained as

$$\frac{\delta\Gamma[\phi, \Delta]}{\delta\phi_x^i} = -J_x^i - K_{xy}^{ij} \phi_y^j, \quad \frac{\delta\Gamma[\phi, \Delta]}{\delta\Delta_{xy}^{ij}} = -\frac{i}{2} K_{xy}^{ij}. \quad (2.8)$$

In the limit of vanishing external sources, the physical solution is obtained by extremizing the 2PI effective action $\Gamma[\phi, \Delta]$. In particular, the EoM for the propagator has the form

$$\Delta^{-1} = \Delta^{(0)-1}[\phi] + \Pi[\phi, \Delta], \quad (2.9)$$

where $\Pi[\phi, \Delta]$ is the 1PI self-energy, in which the propagator lines are given by the dressed propagator matrix Δ . When a given truncation of $\Gamma[\phi, \Delta]$ is explicitly considered, this EoM implicitly resums an infinite set of perturbation-theory Feynman graphs, as shown in Fig. 1.

By considering the $\mathbb{O}(N)$ invariance of the 2PI effective action $\Gamma[\phi, \Delta]$ we may find a WI valid in the 2PI formalism at the extremal point of the 2PI effective action [20]:

$$v \int_x \frac{\delta^2\Gamma[\phi, \Delta]}{\delta G_x \delta G_y} + 2 \frac{\delta^2\Gamma[\phi, \Delta]}{\delta G_y \delta \Delta_{xz}^{GH}} \left(\Delta_{xz}^{HH} - \Delta_{xz}^{GG} \right) = 0. \quad (2.10)$$

When $\mathbb{O}(N)$ -symmetric truncations of the 2PI effective action are considered, the approximate solutions ϕ_x^i and Δ_{xy}^{ij} satisfy (2.10), which is the WI of the 2PI formalism, but not, in general, the Goldstone theorem, which is a WI of the 1PI formalism. Unlike the latter, the WI (2.10) does not protect the masslessness of the Goldstone boson. In fact, as it has explicitly been shown in [17, 18, 19], the Goldstone boson G is not massless in the HF approximation, manifesting itself as a pole at $k^2 \neq 0$ in the Goldstone-boson propagator $\Delta^{GG}(k)$. We stress here that the exact solutions obtained from the *complete* 2PI effective action satisfy, instead, the Goldstone theorem, since the complete 1PI and 2PI effective actions are fully equivalent at their extremal points [4].

3. Symmetry-improved 2PI Effective Action

In this section we present the symmetry-improved formalism for the 2PI effective action $\Gamma[\phi, \Delta]$, which respects the Goldstone theorem for any $\mathbb{O}(N)$ -symmetric truncation of $\Gamma[\phi, \Delta]$.

From the discussion in the previous section, it is clear that when a given truncation of the 2PI effective action $\Gamma_{\text{tr}}[\phi, \Delta]$ is considered, the solution obtained extremizing $\Gamma_{\text{tr}}[\phi, \Delta]$ with respect to ϕ and Δ fails to satisfy the Goldstone theorem

$$v \int_x \Delta_{xy}^{-1, GG} = v \Delta^{-1, GG}(k) \Big|_{k=0} = 0. \quad (3.1)$$

The symmetry-improved EoMs are obtained by imposing the 1PI WI (3.1) directly as a constraint for the Goldstone propagator. This can be achieved, in a variational formulation, by performing a constrained extremization of the 2PI effective action, i.e. by finding the extremum of

$$\tilde{\Gamma}[\phi, \Delta, \ell] = \Gamma_{\text{tr}}[\phi, \Delta] - \ell_y^0 \phi_x^H \Delta_{xy}^{-1, GG}, \quad (3.2)$$

where ℓ_x^0 is a Lagrange-multiplier field. In [20] it is shown that this procedure results in replacing the 2PI EoM with the 1PI one

$$\frac{\delta\Gamma_{\text{tr}}[\phi, \Delta]}{\delta\phi_x^H} = 0 \quad \longrightarrow \quad \frac{\delta\Gamma_{\text{1PI}}[\phi]}{\delta\phi_x^H} = 0. \quad (3.3)$$

The latter is explicitly given by the 1PI WI

$$\frac{\delta\Gamma_{\text{1PI}}[\phi]}{\delta\phi_x^H} = \phi_x^H \Delta_{xy}^{-1,GG}[\phi]. \quad (3.4)$$

Therefore, assuming homogeneity, the symmetry-improved EoMs to solve in the SSB phase are

$$\frac{\delta\Gamma_{\text{tr}}[v, \Delta]}{\delta\Delta^{ij}(k)} = 0, \quad (3.5a)$$

$$v \Delta^{-1,GG}(k) \Big|_{k=0} = 0, \quad (3.5b)$$

namely the standard 2PI EoM for the propagators and the Goldstone theorem itself. In the symmetric phase of the theory we have $v = 0$ and only (3.5a) needs to be solved.

For homogeneous background field values ϕ away from the minimum v , i.e. for $\phi \neq v$, we may define a symmetry-improved effective potential $\tilde{V}_{\text{eff}}(\phi)$ by means of the 1PI WI (3.4), seen as a differential equation defining the improved potential. We thus have the definition [20]

$$- \frac{d\tilde{V}_{\text{eff}}(\phi)}{d\phi} \equiv \phi \Delta^{-1,GG}(k=0; \phi), \quad (3.6)$$

where $\Delta^{-1,GG}(k=0; \phi)$ is the Goldstone component of the solution of the EoM for the propagators (3.5a) for generic $\phi \neq v$. This definition is manifestly compatible with the EoMs at $\phi = v$ (3.5). The integral form of (3.6) is

$$\tilde{V}_{\text{eff}}(\phi) = - \int_0^\phi d\phi \phi \Delta^{-1,GG}(k=0; \phi) + \tilde{V}_{\text{eff}}(\phi=0). \quad (3.7)$$

We show in [20] that the additive constant $\tilde{V}_{\text{eff}}(\phi=0)$ can be chosen such that the formalism is thermodynamically consistent in the sense discussed first by Baym in [27]. However, for the purposes of this work, we do not need to determine it. We refer the interested reader to [20] for a more detailed discussion.

4. The Hartree-Fock Approximation

In this section we apply the symmetry-improved approach outlined in the previous section to the HF approximation of the 2PI effective action. We show that the predicted Goldstone boson is massless, as it should be, and that the phase-transition is second order already in this approximation. These predictions are in agreement with general field-theoretic properties that hold for the full effective action of the theory, thus showing that the symmetry-improved formalism gives actually *improved* predictions as compared to the standard truncated effective action.

The HF approximation consists in retaining only the *double-bubble* graphs (a)–(c) of Fig. 2. The unrenormalized 2PI effective action in this approximation is given by

$$\begin{aligned} \Gamma_{\text{HF}}[v, \Delta^H, \Delta^G] &= \int_x \left(\frac{m^2}{2} v^2 - \frac{\lambda}{4} v^4 \right) - \frac{i}{2} \text{Tr} \left(\ln \Delta^H \right) - \frac{i}{2} \text{Tr} \left(\ln \Delta^G \right) \\ &+ \frac{i}{2} \text{Tr} \left(\Delta^{(0)-1,H} \Delta^H \right) + \frac{i}{2} \text{Tr} \left(\Delta^{(0)-1,G} \Delta^G \right) \\ &- i \frac{-6i\lambda}{8} i\Delta_{xx}^H i\Delta_{xx}^H - i \frac{-2i\lambda}{4} i\Delta_{xx}^H i\Delta_{xx}^G - i \frac{-6i\lambda}{8} i\Delta_{xx}^G i\Delta_{xx}^G, \quad (4.1) \end{aligned}$$

$$\Gamma^{(2)} = \begin{array}{c} \text{H} \\ \bigcirc \\ \text{H} \\ (a) \end{array} + \begin{array}{c} \text{G} \\ \bigcirc \\ \text{G} \\ (b) \end{array} + \begin{array}{c} \text{H} \\ \bigcirc \\ \text{G} \\ (c) \end{array} + \begin{array}{c} \text{H} \\ \bigcirc \\ \text{H} \\ (d) \end{array} + \begin{array}{c} \text{G} \\ \bigcirc \\ \text{H} \\ (e) \end{array}$$

Figure 2. Unrenormalized two-loop contributions to $\Gamma[\phi, \Delta]$, with thick lines denoting dressed propagators. The HF approximation consists of the graphs (a), (b) and (c) and the sunset approximation includes the graphs (d) and (e).

In the above, we have simplified the notation for the diagonal propagators as $\Delta^H \equiv \Delta^{HH}$ and $\Delta^G \equiv \Delta^{GG}$.

4.1. Renormalization

It has been shown in [28, 29, 30] that the 2PI effective action is renormalizable with temperature-independent counterterms (CTs).

To renormalize the theory, we consider all parameters occurring in the CJT effective action (4.1) to be bare (denoted with the subscript B):

$$\phi_B^i = Z^{1/2} \phi^i, \quad m_B^2 = Z^{-1}(m^2 + \delta m^2), \quad \lambda_B = Z^{-2}(\lambda + \delta\lambda), \quad \Delta_B^{ij} = Z \Delta^{ij}. \quad (4.2)$$

In the 2PI formalism, there are two distinct 2-point operators appearing in the effective actions, corresponding to the two different derivatives

$$\frac{\delta^2 \Gamma_{\text{tr}}[\phi, \Delta]}{\delta\phi \delta\phi}, \quad \frac{\delta \Gamma_{\text{tr}}[\phi, \Delta]}{\delta\Delta}, \quad (4.3)$$

When a generic truncation of $\Gamma[\phi, \Delta]$ is considered, these two operators are independent (including their divergences), and need to be renormalized by two different CTs [30]. Analogously, in the truncated 2PI formalism we have the independent 4-point functions

$$\frac{\delta^4 \Gamma_{\text{tr}}[\phi, \Delta]}{\delta\phi \delta\phi \delta\phi \delta\phi}, \quad \frac{\delta^3 \Gamma_{\text{tr}}[\phi, \Delta]}{\delta\phi \delta\phi \delta\Delta}, \quad \frac{\delta^2 \Gamma_{\text{tr}}[\phi, \Delta]}{\delta\Delta \delta\Delta}. \quad (4.4)$$

Moreover, in the $\mathbb{O}(N)$ model these operators appear in two different $\mathbb{O}(N)$ -invariant combinations, denoted by A and B . It is shown in [30] that only the standard perturbation-theory coupling-constant CT $\delta\lambda$ is required to renormalize the higher-loop graphs of the 2PI effective action, when going beyond the HF approximation. Hence, a finite number of CTs is needed to make the effective action finite, thus guaranteeing its renormalizability. With the

above considerations, the effective action (4.1) reads:

$$\begin{aligned}
\Gamma_{\text{HF}}[v, \Delta^H, \Delta^G] &= \int_x \left(\frac{m^2 + \delta m_0^2}{2} v^2 - \frac{\lambda + \delta \lambda_0}{4} v^4 \right) - \frac{i}{2} \text{Tr} \left(\ln \Delta^H \right) - \frac{i}{2} \text{Tr} \left(\ln \Delta^G \right) \\
&- \frac{i}{2} \text{Tr} \left\{ \left[Z \partial^2 + \left(3\lambda + \delta \lambda_1^A + 2\delta \lambda_1^B \right) v^2 - \left(m^2 + \delta m_1^2 \right) \right] \Delta^H \right\} \\
&- \frac{i}{2} \text{Tr} \left\{ \left[Z \partial^2 + \left(\lambda + \delta \lambda_1^A \right) v^2 - \left(m^2 + \delta m_1^2 \right) \right] \Delta^G \right\} \\
&- i \frac{-i(3\lambda + \delta \lambda_2^A + 2\delta \lambda_2^B)}{4} i \Delta_{xx}^H i \Delta_{xx}^H - i \frac{-2i(\lambda + \delta \lambda_2^A)}{4} i \Delta_{xx}^H i \Delta_{xx}^G \\
&- i \frac{-i(3\lambda + \delta \lambda_2^A + 2\delta \lambda_2^B)}{4} i \Delta_{xx}^G i \Delta_{xx}^G, \tag{4.5}
\end{aligned}$$

where we may set $Z = 1$ at this order of loop expansion.

By canceling separately divergences and subdivergences proportional to temperature-dependent terms, in [20] we find the following CTs in the HF approximation, in the $\overline{\text{MS}}$ scheme of dimensional regularization $d = 4 - 2\epsilon$:

$$\delta \lambda_2^A = \delta \lambda_1^A = \frac{2\lambda^2}{16\pi^2\epsilon} \frac{3 - \frac{4\lambda}{16\pi^2\epsilon}}{1 - \frac{6\lambda}{16\pi^2\epsilon} + \frac{8\lambda^2}{(16\pi^2\epsilon)^2}}, \tag{4.6a}$$

$$\delta \lambda_2^B = \delta \lambda_1^B = \frac{2\lambda^2}{16\pi^2\epsilon} \frac{1}{1 - \frac{2\lambda}{16\pi^2\epsilon}}, \quad \delta m_1^2 = \frac{4\lambda m^2}{16\pi^2\epsilon} \frac{1}{1 - \frac{4\lambda}{16\pi^2\epsilon}}. \tag{4.6b}$$

The above $T = 0$ CTs are sufficient to renormalize the EoMs for the propagators, also when thermal effects are considered.

4.2. Thermal Phase Transition

In the HF approximation, the self-energies are momentum independent. Therefore, we may parameterize the propagators as $\Delta^{H/G}(k) = (k^2 - M_{H/G}^2 + i\varepsilon)^{-1}$, where the effective Higgs and Goldstone masses, M_H^2 and M_G^2 , depend only on the temperature T .

In the symmetric phase of the theory the constraint (3.5b) is automatically satisfied, and the renormalized EoMs (3.5a) take on the form

$$M_H^2 = -m^2 + 3\lambda \frac{M_H^2}{16\pi^2} \ln \frac{M_H^2}{2m^2} + \lambda \frac{M_G^2}{16\pi^2} \ln \frac{M_G^2}{2m^2} + 3\lambda \int_{\mathbf{k}} \frac{n(\omega_{\mathbf{k}}^H)}{\omega_{\mathbf{k}}^H} + \lambda \int_{\mathbf{k}} \frac{n(\omega_{\mathbf{k}}^G)}{\omega_{\mathbf{k}}^G}, \tag{4.7a}$$

$$M_G^2 = -m^2 + \lambda \frac{M_H^2}{16\pi^2} \ln \frac{M_H^2}{2m^2} + 3\lambda \frac{M_G^2}{16\pi^2} \ln \frac{M_G^2}{2m^2} + \lambda \int_{\mathbf{k}} \frac{n(\omega_{\mathbf{k}}^H)}{\omega_{\mathbf{k}}^H} + 3\lambda \int_{\mathbf{k}} \frac{n(\omega_{\mathbf{k}}^G)}{\omega_{\mathbf{k}}^G}, \tag{4.7b}$$

where $\int_{\mathbf{k}} \equiv \int d^3\mathbf{k}/(2\pi)^3$, $\omega_{\mathbf{k}} = \sqrt{\mathbf{k}^2 + M^2}$ is the on-shell energy of the (quasi)particle, and $n(\omega) = (e^{\omega/T} - 1)^{-1}$ is the Bose–Einstein distribution function. In the symmetric phase we obtain, as expected, a single solution with $M_G^2 = M_H^2$.

In the HF approximation the constraint (3.5b) reads

$$v M_G^2 = 0. \tag{4.8}$$

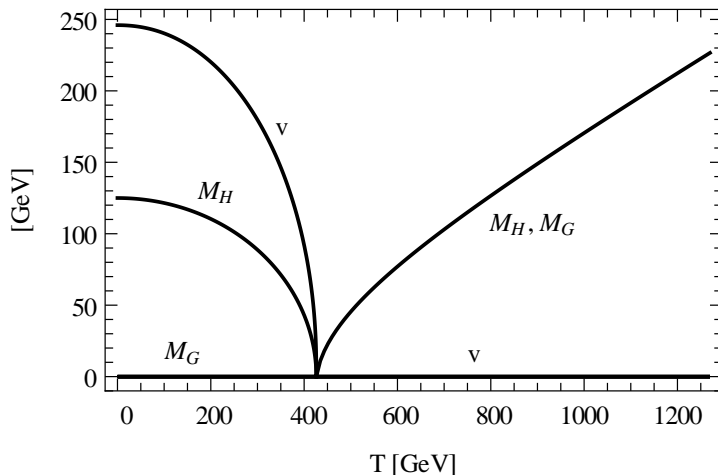


Figure 3. The values of M_H^2 , M_G^2 and the VEV v , as functions of T , predicted in the HF approximation of the symmetry-improved 2PI formalism.

In the SSB phase of the theory this implies $M_G^2 = 0$, yielding the EoMs [20]

$$M_H^2 = 3\lambda v^2 - m^2 + 3\lambda \frac{M_H^2}{16\pi^2} \ln \frac{M_H^2}{2m^2} + 3\lambda \int_{\mathbf{k}} \frac{n(\omega_{\mathbf{k}}^H)}{\omega_{\mathbf{k}}^H} + \lambda \int_{\mathbf{k}} \frac{n(\omega_{\mathbf{k}}^G)}{\omega_{\mathbf{k}}^G}, \quad (4.9a)$$

$$0 = \lambda v^2 - m^2 + \lambda \frac{M_H^2}{16\pi^2} \ln \frac{M_H^2}{2m^2} + \lambda \int_{\mathbf{k}} \frac{n(\omega_{\mathbf{k}}^H)}{\omega_{\mathbf{k}}^H} + 3\lambda \int_{\mathbf{k}} \frac{n(\omega_{\mathbf{k}}^G)}{\omega_{\mathbf{k}}^G}, \quad (4.9b)$$

We point out that we have chosen the $\overline{\text{MS}}$ mass scale μ such that the tree-level relations $M_H^2 = 2m^2$, $v^2 = m^2/\lambda$ are satisfied at $T = 0$. The mass-gap equations (4.9) are solved analytically to be

$$M_H^2 = 2m^2 - \frac{8\lambda T^2}{12}, \quad (4.10a)$$

$$M_G^2 = 0, \quad (4.10b)$$

$$v^2 = \frac{m^2}{\lambda} - \frac{M_H^2}{16\pi^2} \ln \frac{M_H^2}{2m^2} - \int_{\mathbf{k}} \frac{n(\omega_{\mathbf{k}}^H)}{\omega_{\mathbf{k}}^H} - \frac{3T^2}{12}. \quad (4.10c)$$

In Fig. 3, we exhibit the dependence of the squared thermal masses, M_H^2 and M_G^2 , and the thermally-corrected VEV v , as functions of the temperature T . The parameters of the model are chosen such that $M_H = 125$ GeV and $v = 246$ GeV at $T = 0$. We observe that we predict a second-order phase transition at $T = T_c = \sqrt{3}v(T = 0)$, already in the HF approximation, in agreement with theoretical expectations to all orders. This is in sharp contrast with the incorrect first-order phase-transition predicted in the HF approximation by the previous approaches [31, 32, 33].

4.3. Symmetry-improved Effective Potential

Let us now calculate the effective potential at high temperatures in the HF approximation of the symmetry-improved formalism. Extending the renormalized EoMs (4.9) from $v \rightarrow \phi$, we obtain

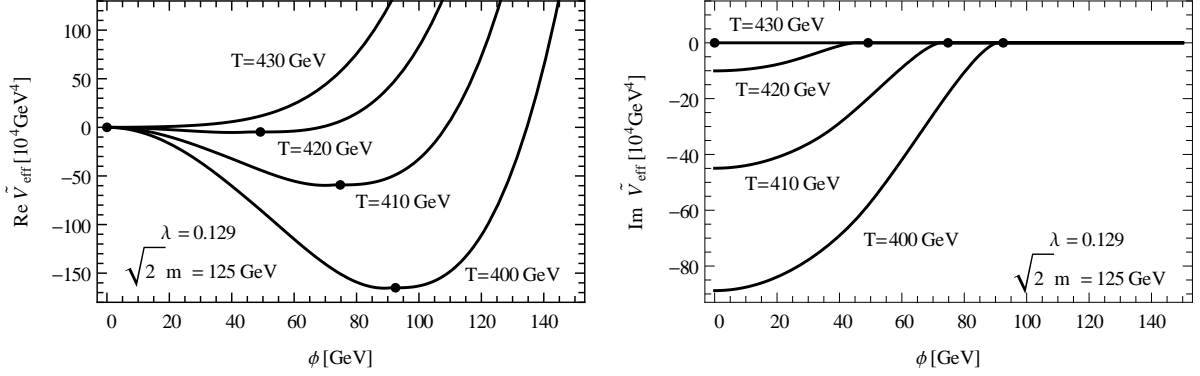


Figure 4. Symmetry-improved HF effective potential in the high-temperature approximation. The large dots denote the minimum solutions $\phi = v$, obtained in Section 4.2.

$$\begin{aligned}
M_H^2(\phi) &= 3\lambda\phi^2 - m^2 + 3\lambda \frac{M_H^2(\phi)}{16\pi^2} \ln\left(\frac{M_H^2(\phi)}{2m^2}\right) + \lambda \frac{M_G^2(\phi)}{16\pi^2} \ln\left(\frac{M_G^2(\phi)}{2m^2}\right) \\
&\quad + 3\lambda \int_{\mathbf{k}} \frac{n[\omega_{\mathbf{k}}^H(\phi)]}{\omega_{\mathbf{k}}^H(\phi)} + \lambda \int_{\mathbf{k}} \frac{n[\omega_{\mathbf{k}}^G(\phi)]}{\omega_{\mathbf{k}}^G(\phi)}, \tag{4.11a}
\end{aligned}$$

$$\begin{aligned}
M_G^2(\phi) &= \lambda\phi^2 - m^2 + \lambda \frac{M_H^2(\phi)}{16\pi^2} \ln\left(\frac{M_H^2(\phi)}{2m^2}\right) + 3\lambda \frac{M_G^2(\phi)}{16\pi^2} \ln\left(\frac{M_G^2(\phi)}{2m^2}\right) \\
&\quad + \lambda \int_{\mathbf{k}} \frac{n[\omega_{\mathbf{k}}^H(\phi)]}{\omega_{\mathbf{k}}^H(\phi)} + 3\lambda \int_{\mathbf{k}} \frac{n[\omega_{\mathbf{k}}^G(\phi)]}{\omega_{\mathbf{k}}^G(\phi)}, \tag{4.11b}
\end{aligned}$$

$$\frac{1}{\phi} \frac{d\tilde{V}_{\text{eff}}(\phi)}{d\phi} = M_G^2(\phi). \tag{4.11c}$$

The first two equations are the EoMs for the propagators, for general $\phi \neq v$. The latter equation (4.11c) results from the definition of the symmetry-improved effective potential (3.6), i.e. the 1PI WI for $\phi \neq v$. Figure 4 presents our numerical estimates for the high-temperature symmetry-improved effective potential, as functions of ϕ , for different temperatures T [20]. Again, a second-order phase transition is described, already in the HF approximation. The fact that $\tilde{V}_{\text{eff}}(\phi)$ acquires an imaginary part when $\phi < v$ signals the instability of the homogeneous vacuum in this region [34].

5. Threshold Properties

In this section, we study the threshold properties of the Higgs and Goldstone particles, by including the contributions from the sunset diagrams (d) and (e) in Fig. 2. In particular, we will show that the resummed Higgs- and Goldstone-boson propagators predicted within our symmetry-improved CJT formalism exhibit the correct threshold properties arising from on-shell Higgs and Goldstone particles in the loop. Therefore, we explicitly demonstrate that the symmetry-improved approach is consistent with the optical theorem and unitarity.

One of the common approaches in the literature, when studying the issue of symmetries in the CJT formalism, is to define an additional 2-point function as

$$\Delta_{\text{ext}}^{-1} \equiv \frac{\delta^2 \Gamma_{\text{tr}}[\phi, \Delta(\phi)]}{\delta\phi \delta\phi}, \tag{5.1}$$

$$\begin{aligned}
i \Delta^{-1,H}(p) &= i \Delta^{(0)-1,H}(p) + \text{---} \bigcirc \text{---} + \text{---} \bigcirc \text{---} + \text{---} \bigcirc \text{---} + \text{---} \bigcirc \text{---} \\
&\quad \begin{array}{c} H \\ \bigcirc \\ H \end{array} \quad \begin{array}{c} G \\ \bigcirc \\ G \end{array} \quad \begin{array}{c} H \\ \bigcirc \\ H \end{array} \quad \begin{array}{c} G \\ \bigcirc \\ G \end{array} \\
i \Delta^{-1,G}(p) &= i \Delta^{(0)-1,G}(p) + \text{---} \bigcirc \text{---} + \text{---} \bigcirc \text{---} + \text{---} \bigcirc \text{---} \\
&\quad \begin{array}{c} H \\ \bigcirc \\ H \end{array} \quad \begin{array}{c} G \\ \bigcirc \\ G \end{array} \quad \begin{array}{c} H \\ \bigcirc \\ G \end{array}
\end{aligned}$$

Figure 5. Higgs and Goldstone EoMs in the sunset approximation.

where $\Delta(\phi)$ is the solution of the standard 2PI EoM for the propagator. This 2-point function is sometimes referred to as the *external propagator*. It can be shown that this function satisfies the Goldstone theorem, since the second derivative (in the Goldstone direction) of any symmetric ϕ -only functional does so [20]. Thus, it is often claimed that this function should be considered as the true approximation to the propagator, in the CJT formalism, rather than Δ . However, the problem of this approach is that what appears in the diagrammatic series of $\Gamma[\phi, \Delta]$ is the propagator Δ , not the external propagator Δ_{ext} . The former does not satisfy the Goldstone theorem, in the standard CJT formalism, and therefore the thresholds of the particles are described incorrectly, since the Goldstone bosons propagating within quantum loops are massive. In this sense, this approach is not capable of describing the Goldstone bosons as consistently massless quantum-mechanically, i.e. within loops. From the above discussion, it is clear that studying the threshold properties described by the symmetry-improved 2PI effective action is an important step in establishing the consistency of the formalism and show further its advantages as compared to previous approaches.

As diagrammatically represented in Fig. 5, the symmetry-improved 2PI EoMs derived in the sunset approximation are given by

$$\begin{aligned}
\Delta^{-1,H}(p) &= p^2 - (3\lambda + \delta\lambda_1^A + 2\delta\lambda_1^B)v^2 + m^2 + \delta m_1^2 - (3\lambda + \delta\lambda_2^A + 2\delta\lambda_2^B)\mathcal{T}_H \\
&\quad - (\lambda + \delta\lambda_2^A)\mathcal{T}_G + \frac{1}{i} \frac{(-6i\lambda v)^2}{2} \mathcal{I}_{HH}(p) + \frac{1}{i} \frac{(-2i\lambda v)^2}{2} \mathcal{I}_{GG}(p), \quad (5.2a)
\end{aligned}$$

$$\begin{aligned}
\Delta^{-1,G}(p) &= p^2 - (\lambda + \delta\lambda_1^A)v^2 + m^2 + \delta m_1^2 \\
&\quad - (\lambda + \delta\lambda_2^A)\mathcal{T}_H - (3\lambda + \delta\lambda_2^A + 2\delta\lambda_2^B)\mathcal{T}_G + \frac{1}{i} (-2i\lambda v)^2 \mathcal{I}_{HG}(p), \quad (5.2b)
\end{aligned}$$

$$v \Delta^{-1,G}(0) = 0. \quad (5.2c)$$

Here, we have abbreviated the loop integrals as follows:

$$\mathcal{T}_a = \bar{\mu}^{2\epsilon} \int_k i\Delta^a(k), \quad \mathcal{I}_{ab}(p) = \bar{\mu}^{2\epsilon} \int_k i\Delta^a(k-p) i\Delta^b(k), \quad (5.3)$$

where $a, b = H, G$, $\ln \bar{\mu}^2 = \ln \mu^2 + \gamma - \ln(4\pi)$ and μ is the $\overline{\text{MS}}$ renormalization scale. In (5.2) we have introduced the shorthand notation $\int_k \equiv \int d^4k / (2\pi)^4$. Details of the renormalization and the numerical approach to solve these self-consistent nonlinear equations are given in [20]. Here, we only outline the physical content of their solution.

It is useful to define the effective energy-dependent squared masses $\widehat{M}_{H/G}^2(s)$ as

$$\Delta^{-1,H/G}(s) = s - \widehat{M}_{H/G}^2(s), \quad (5.4)$$

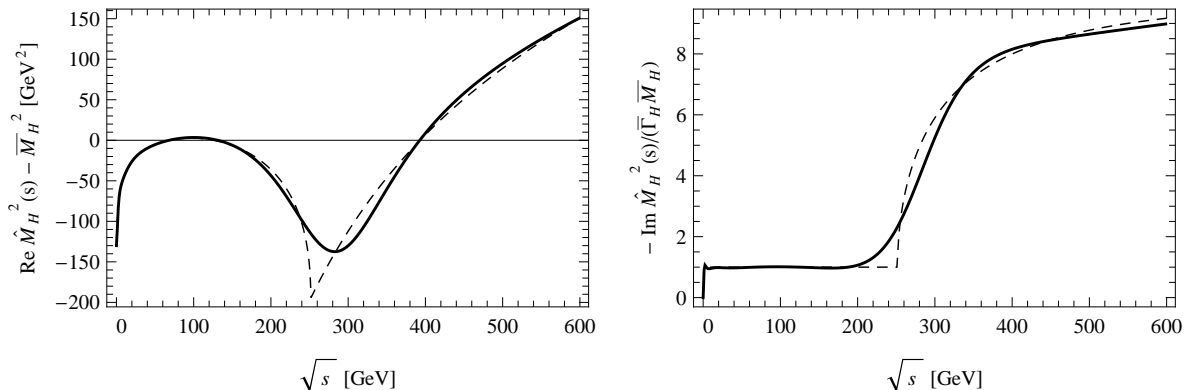


Figure 6. Numerical solutions for $\text{Re}[\widehat{M}_H^2(s)] - \overline{M}_H^2$ (left frame) and $\text{Im}[\widehat{M}_H^2(s)]/(\overline{\Gamma}_H \overline{M}_H)$ (right frame), where \overline{M}_H and $\overline{\Gamma}_H$ are the Higgs-boson pole mass and width, respectively. The dashed lines are the one-loop results in the 1PI formalism.

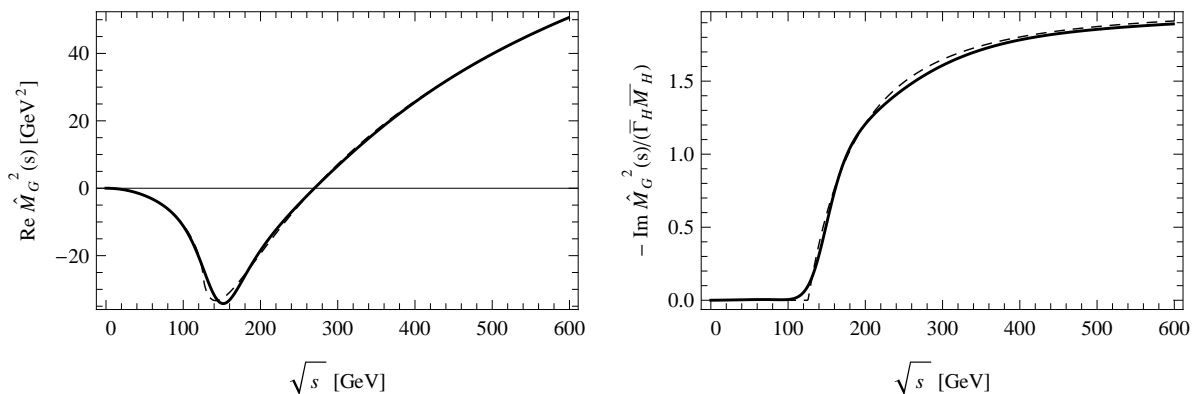


Figure 7. Numerical solutions for $\text{Re}[\widehat{M}_G^2(s)]$ (left frame) and $\text{Im}[\widehat{M}_G^2(s)]/(\overline{\Gamma}_H \overline{M}_H)$ (right frame).

where $s \equiv p^2$ is the Lorentz-invariant energy-squared parameter. In Fig. 6 and Fig. 7, we plot the dispersive (real) and absorptive (imaginary) Higgs- and Goldstone-boson mass squares, as functions of s . We see that there is a non-vanishing absorptive part $\text{Im}[\widehat{M}_H^2(s)]$ that results from the on-shell decay of the Higgs particle into two Goldstone bosons, i.e. $H \rightarrow GG$. The threshold for this process is at $s = 0$, thus demonstrating that *the Goldstone bosons in the loop are consistently treated as massless within our symmetry-improved 2PI formalism*. This is, again, in sharp contrast with previous approaches in the literature, e.g. with the results found in [31] for the absorptive part of the external propagator, where the Goldstone boson exhibits a non-zero mass in the loop, as discussed above.

The dashed lines in Figs. 6 and 7 show the predictions obtained at one-loop level in the 1PI formalism. We point out that the kinematic opening of the thresholds is very sharp, as opposed to the smooth thresholds predicted by our symmetry-improved CJT formalism. As illustrated in Fig. 8 this is due to the fact that *the 2PI formalism automatically resums infinitely-many higher-order processes, without the need of explicitly considering them*, including also processes that take place below the 1PI threshold.

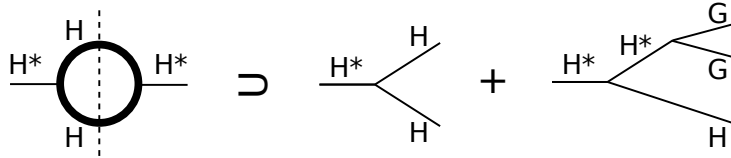


Figure 8. Some of the on-shell processes whose description is included in the absorptive part of the 1-loop CJT self-energy on the LHS.

6. The Infrared Divergences of the Standard-Model Effective Potential

In this section we describe the issue, recently pointed out in [23], of the IR divergences of the SM effective potential due to the Goldstone bosons of the electroweak group. Then, by considering the scalar sector of the SM, we show how the symmetry-improved 2PI effective action can be used to study this problem, and compare the results obtained in this framework with the existing approach [24, 25] in the literature. More technical details of the 2PI analysis will be given in a forthcoming publication [26].

The effective potential V_{eff} of the SM, calculated in perturbation theory, suffers from IR divergences due to the appearance of Goldstone bosons in ring diagrams, as shown in Figure 9. At 3 loops the divergence is logarithmic, but it becomes more and more severe with increasing loop order. Moreover, these divergences are more severe when one considers the derivative of the effective potential $\frac{dV_{\text{eff}}}{d\phi}$. For the latter, IR divergences start from 2-loop order (see Figure 9).

In perturbation theory these divergences appear when the tree-level Goldstone propagators become massless, i.e. at the tree-level minimum of the potential. This is instead finite, together with its derivatives, at the dressed minimum $\phi = v$. Nevertheless, this problem needs to be addressed, for the following reasons:

- (i) The effective potential $V_{\text{eff}}(\phi)$ should be well-defined for all values of ϕ , not only at its minimum $\phi = v$. Among other things, the off-shell $\phi \neq v$ effective potential governs the dynamics of the background field in inflationary scenarios.
- (ii) At the dressed minimum $\phi = v$, the dressed masses of the Goldstone bosons vanish, and this implies that the tree-level mass m_G^2 is formally of the same order as the 1-loop Goldstone self-energy $\Pi_G^{(1)}$. Thus, since starting from 3-loop order the IR divergences of $\frac{dV_{\text{eff}}}{d\phi}$ are of the form $1/(m_G^2)^n$, $n \geq 1$ (see Figure 9) all *these higher-loop contributions to $\frac{dV_{\text{eff}}}{d\phi}$ are formally at 2-loop order*. This means that perturbation theory breaks down and these diagrams can potentially have a significant impact on 2-loop results for $\frac{dV_{\text{eff}}}{d\phi}$, i.e. on the state-of-the-art threshold corrections to the VEV v . In view of the extreme sensitivity of the SM effective potential, extrapolated at very high energies, to the matching conditions at the electroweak scale [1, 2, 3], these issues can potentially affect the stability analyses of the SM.

Moreover, a seemingly unrelated problem is that the tree-level mass of the Goldstone boson can be negative at the dressed minimum $\phi = v$, thus generating an unphysical imaginary part for the SM effective potential at its minimum, which does not correspond to a true instability of the homogeneous vacuum. This fact should be contrasted with the discussion in Section 3, where we have shown that the symmetry-improved effective potential acquires an imaginary part only in the concave region corresponding to a physical instability. This suggests that a resummation of higher-loop diagrams is needed to address this conceptual issue as well.

Finally, we point out that the location of the IR divergence depends on the value of the gauge-fixing parameter ξ , but the divergence is nonetheless present in any renormalizable R_ξ gauge at the value of the field ϕ for which $m_G^2(\phi; \xi) = 0$.

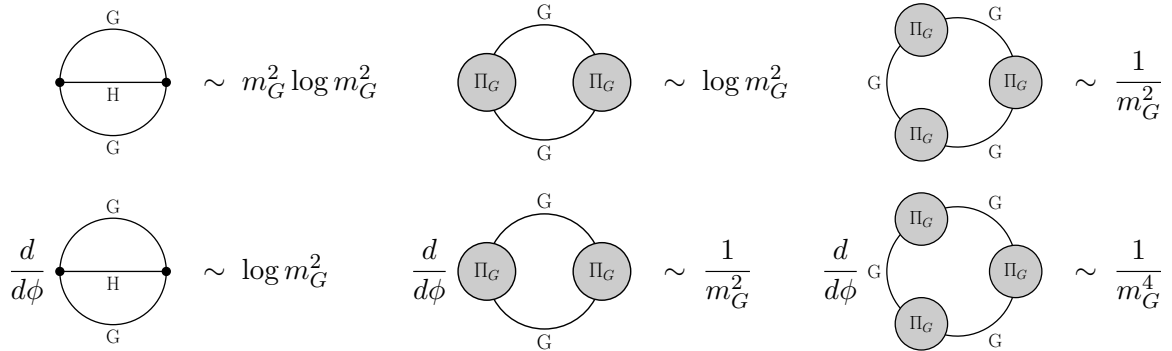


Figure 9. IR behaviour of Goldstone-boson ring diagrams contributing to the effective potential and its derivative. The IR divergences start at three loops for $V_{\text{eff}}(\phi)$, already at two loops for its derivative $dV_{\text{eff}}/d\phi$.

6.1. Approximate Partial Resummation

Let us outline the approximate partial resummation procedure presented in [24, 25] to address these IR issues. To facilitate an objective comparison with the 2PI approach discussed in this work, we will limit ourselves to the scalar sector of the SM, i.e. we will consider a global $\text{SU}(2) \times \text{U}(1)$ model with only the scalar Higgs doublet. Although this does not allow to draw quantitative conclusion for the complete SM case, this simplified model is sufficient to study this issue qualitatively and to compare the results obtained in the 2PI approach with the ones in [24, 25].

The partial resummation procedure consists in considering ring diagrams, as in Figure 9, with insertions of 1-loop Goldstone self-energies $\Pi_G(k)$. One approximates these 1-loop self-energies with their zero-momentum value $\Pi_G(0)$. With this important simplification, one can resum these diagrams by replacing the 1-loop Coleman-Weinberg contribution of the Goldstone bosons with

$$V_{\text{eff},G}^{(1)} = \frac{3m_G^4}{4(16\pi^2)} \left[\log\left(\frac{m_G^2}{\mu^2}\right) - \frac{3}{2} \right] \longrightarrow \frac{3(m_G^2 + \Pi_G(0))^2}{4(16\pi^2)} \left[\log\left(\frac{m_G^2 + \Pi_G(0)}{\mu^2}\right) - \frac{3}{2} \right]. \quad (6.1)$$

However, it can be shown that the derivative of this resummed term is still divergent. This problem can be solved by limiting $\Pi_G(0)$ to contain only the terms not proportional to m_G^2 , i.e. by replacing

$$\Pi_G(0) \longrightarrow \Pi_g \equiv \Pi_G(0) - \frac{3\lambda}{(16\pi^2)} m_G^2 \left(\log(m_G^2/\mu^2) - 1 \right). \quad (6.2)$$

Notice that the subtracted term does not correspond to the contribution of a given diagram, but it is contained in the contribution of both the Goldstone tadpole integral and the Higgs-Goldstone sunset diagram. Finally, one needs to subtract from V_{eff} the diagrams that would be double-counted otherwise. In conclusion, one adds to the effective potential the term [24, 25]:

$$V_{\text{eff},G}^{(\text{resum})} \equiv \frac{3(m_G^2 + \Pi_g)^2}{4(16\pi^2)} \left[\log\left(\frac{m_G^2 + \Pi_g}{\mu^2}\right) - \frac{3}{2} \right] - V_{\text{eff},G}^{(\text{d.c.})}, \quad (6.3)$$

where $V_{\text{eff},G}^{(\text{d.c.})}$ is the contribution of the double-counted diagrams, as discussed above.

As we show in Figure 10 for the scalar sector of the SM, this procedure effectively resums the IR divergences present in $dV_{\text{eff}}/d\phi$ at two- and three-loop orders. We include only the 3-loop

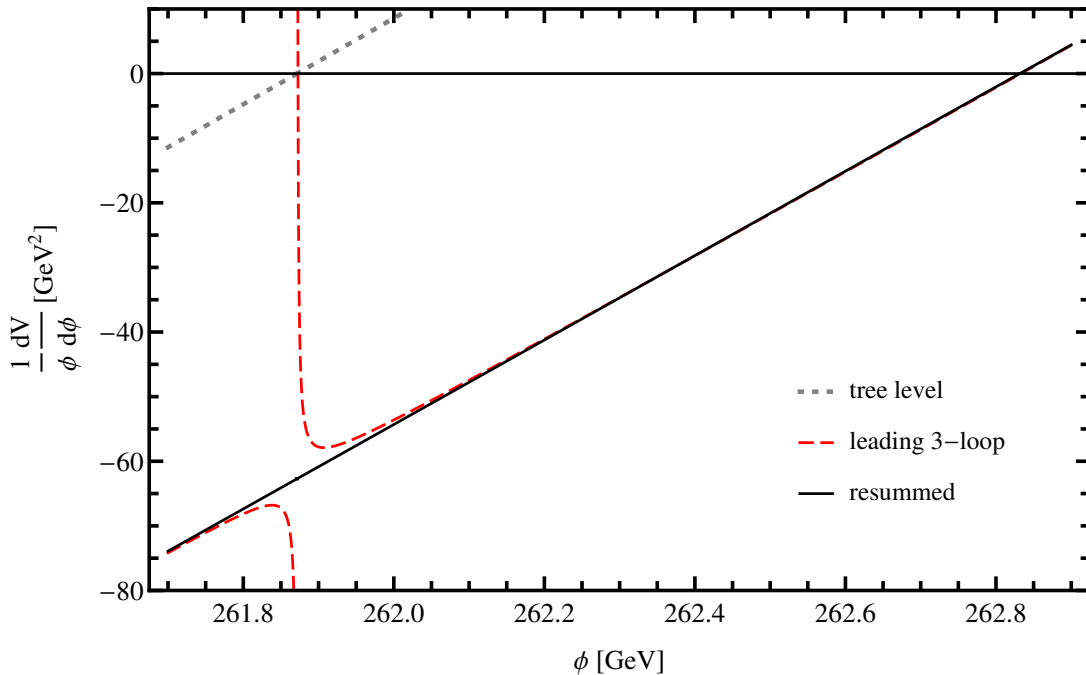


Figure 10. IR divergence of the derivative of the effective potential, as calculated in perturbation theory at 3-loop order, considering only the scalar sector of the SM. The gray dotted line is the tree-level contribution, the red dashed line the leading 3-loop one, whereas the black continuous line is the result of the approximate partial resummation procedure developed in [24, 25].

contributions coming from the Goldstone ring diagrams in Figure 9, since they are proportional to $1/m_G^2$ and so responsible for the IR divergence. Moreover, as we discussed above, their order gets formally lowered at the dressed minimum.

6.2. 2PI Approach to the Resummation of IR Divergences

We now study these issues by means of the symmetry-improved 2PI formalism. This provides a more complete resummation, as compared to the approach outlined above, for several reasons. First, it is a first-principle approach, and no ad-hoc subtraction is needed. Second, as we are going to show below, the 2PI approach takes into account more topologies and does not necessitate to neglect the momentum dependence of the self-energy insertions that are resummed. Moreover, as we showed in the previous section, the threshold properties are correctly described within the symmetry-improved formalism. In particular, the Goldstone propagator in the formalism is massless at the dressed minimum of the potential and nevertheless the effective potential will be shown to be free of IR pathologies.

We consider the global $\text{SU}(2) \times \text{U}(1)$ scalar model. By including, in the EoMs, the 1-loop (HF + sunset) CJT diagrams shown in the first line of Figure 11 we actually resum, automatically, a large class of diagrams, as depicted in Figure 12. Moreover, in order to be able to compare our results with the perturbative 2-loop calculation, we include the 2-loop CJT diagrams in the second line of Figure 11. However, to simplify the treatment, we approximate the propagators appearing in these diagrams as the tree-level ones $\Delta(\phi) \approx \Delta^{(0)}(\phi)$. In this way, we take into account the full contribution of 2-loop topologies and, in addition, resum diagrams as the ones shown in Figure 13. Therefore, a much larger class of diagrams is included, as compared to the

$$\begin{aligned}
\Delta^{-1}(\phi) &= \Delta^{(0)-1}(\phi) + \text{[diagram: tadpole]} + \text{[diagram: self-energy loop]} \\
&+ \left[\text{[diagram: bubble]} + \text{[diagram: sunset]} + \text{[diagram: triangle]} + \text{[diagram: figure-eight]} \right]_{\Delta \approx \Delta_0(\phi)}
\end{aligned}$$

Figure 11. Diagrammatic representation of the approximation scheme for the EoMs in Section 6.

$$\begin{aligned}
\underline{\text{[diagram: bubble]}} + \text{[diagram: self-energy loop]} &= \underline{\text{[diagram: bubble]}} + \text{[diagram: self-energy loop]} + \dots + \text{[diagram: bubble with tadpole]} \\
&+ \dots + \underline{\text{[diagram: bubble with tadpole]}} + \dots + \text{[diagram: bubble with two tadpoles]} + \dots
\end{aligned}$$

Figure 12. Some of the topologies implicitly resummed by the 1-loop 2PI self-energies in the first line of Figure 11.

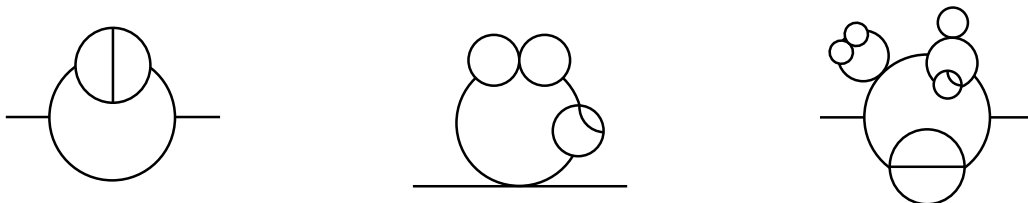


Figure 13. Some examples of the topologies resummed by including the 2-loop 2PI self-energies in the second line of Figure 11. Notice that the propagators belonging to 2-loop 2PI topologies do not get dressed, because of the approximation $\Delta(\phi) \approx \Delta^{(0)}(\phi)$ used, for these, in Figure 11.

method outlined in Section 6.1, and the momentum dependence of the resummed insertions is also retained.

In the symmetry-improved 2PI approach, the IR divergences are absent by construction: IR divergences can be present only when two or more Goldstone propagators carry the same momentum, as in the ring diagrams shown in Figure 9. In other words, the IR pathologies originate from chains of Goldstone lines with self-energy insertions between them. However, such topologies are necessarily *2-particle-reducible* and thus do not appear in the diagrammatic series of $\Gamma[\phi, \Delta]$. Therefore, the resummation of IR divergences is achieved automatically by the construction of the 2PI effective action.

The EoMs can be easily obtained by generalizing (5.2) and including the 2-loop self-energies, in which $\Delta(\phi) \approx \Delta^{(0)}(\phi)$. Their explicit form is given in Appendix A. The numerical solution, in the vicinity of the dressed minimum $\phi = v$, is plotted in Figure 14. The black dots represent the numerical solution obtained in our approach. It is apparent that the results from the partial

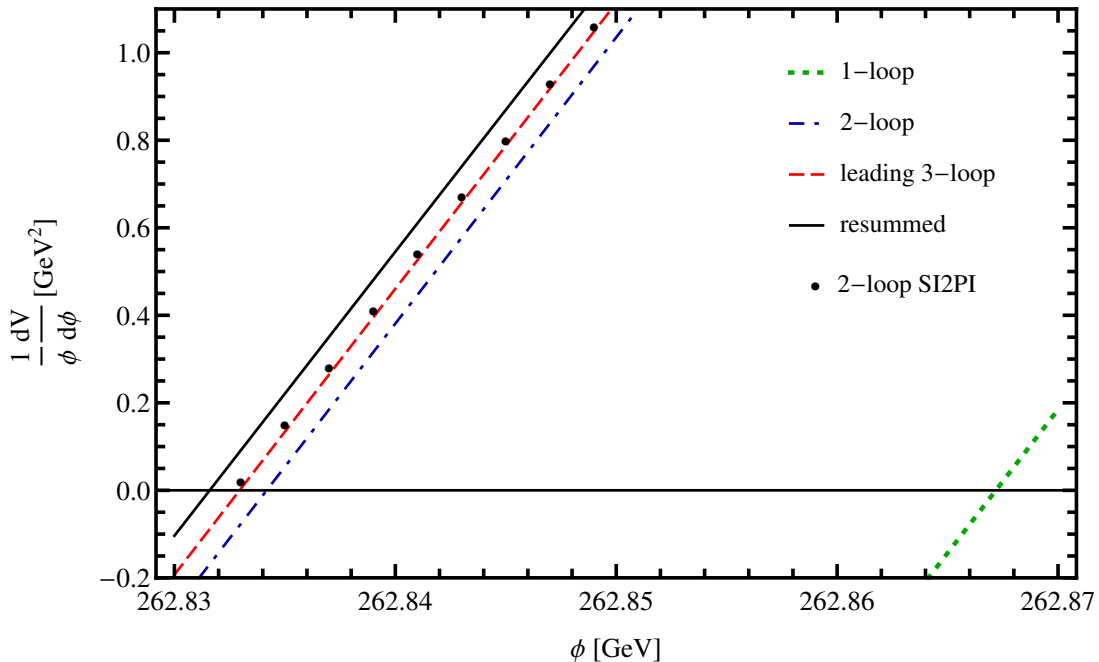


Figure 14. The derivative of the effective potential, near its dressed minimum. We show results from 1-loop (green dotted line), 2-loop (blue dash-dotted line) and leading 3-loop (red dashed line) perturbation theory. The black continuous line is the result of the approximate partial resummation procedure discussed in Section 6.1. The black dots are the results obtained from the symmetry-improved 2PI effective action.

resummation outlined in Section 6.1 do not reproduce the ones obtained in the more complete 2PI resummation. We have checked explicitly that, expanding the EoMs at 2-loop order, we reproduce numerically the results coming from 2-loop perturbation theory. Notice also that the 3-loop result is larger than what one would naively expect (roughly about $\lambda/16\pi^2$ times the 2-loop one), because of the breakdown of perturbation theory, as discussed at the beginning of this section. In Figure 14 the symmetry-improved 2PI solution appears to be similar in size to the leading 3-loop result, potentially indicating that the effect of the resummation is small near the dressed minimum. However, this is a coincidence and depends on the class of topologies of graphs considered here. A more detailed study will be given in [26].

7. Conclusions

The 2PI effective action provides a powerful theoretical tool to consistently resum infinite series of perturbation-theory diagrams of different topologies. However, its loopwise expansion introduces residual violations of possible global symmetries by higher-order terms. In the case of global symmetries, this leads to the appearance of massive Goldstone bosons in the spontaneously broken phase of the theory. In this work we have reviewed the symmetry-improved CJT formalism, developed in [20] for consistently encoding global symmetries in loopwise expansions of the 2PI effective action.

We have demonstrated, in a simple $\mathbb{O}(2)$ scalar model, the key field-theoretical properties of the formalism. In detail, we have shown that the Goldstone bosons are described as massless, also within quantum loops, thus providing a consistent description of the threshold properties of the Higgs and Goldstone particles. Moreover, the thermal phase transition is at second order

already in the HF approximation. Thus, the behaviour expected for the full theory is recovered already in the first non-trivial approximation, contrary to other approaches in the literature.

Thanks to the satisfactory field-theoretical properties of the formalism, we have applied the symmetry-improved 2PI effective action to the study of the IR divergences of the SM effective potential due to the electroweak Goldstone bosons. By limiting ourselves to the scalar sector of the electroweak group, we have confirmed that these IR divergences are indeed an artifact of perturbation theory, and are absent in the symmetry-improved 2PI formalism, as it should be. We have compared quantitatively our results with the predictions given by the existing approach in the literature, consisting in an approximate partial resummation of Goldstone-boson ring diagrams. We have shown that the latter, whilst correctly resumming qualitatively the IR divergences, does not reproduce quantitatively, at least in the simplified scalar model considered here, the results of the more complete 2PI resummation, near the dressed minimum of the effective potential.

In view of the extreme sensitivity of the SM effective potential, extrapolated to very high energies, to the matching conditions at the electroweak scale, it is important to assess these issues in a more realistic way, going beyond the scalar sector of the SM. A detailed study of this matter, including the quantitatively most important contributions, will be given in a forthcoming publication.

Acknowledgments

The work of A.P. is supported by the Lancaster-Manchester-Sheffield Consortium for Fundamental Physics under STFC grant ST/L000520/1. The work of D.T. is supported by a fellowship of the EPS Faculty of the University of Manchester.

Appendix A. Equations of Motion for the $\text{SU}(2) \times \text{U}(1)$ Scalar Model

In this appendix we give the renormalized EoMs used in Section 6.2 to study the IR divergences of the effective potential. Since the scalar $\text{SU}(2)_L \times \text{U}(1)$ model automatically possesses the custodial symmetry $\text{SU}(2)_L \times \text{SU}(2)_R \sim \mathbb{O}(4)$, the HF and sunset contributions to the EoMs are easily inferred from the $\mathbb{O}(2)$ case (see [20]). We find, in Euclidean space:

$$\Delta^{-1,H}(p; \phi) = p^2 + 3\lambda\phi^2 - m^2 + 3\lambda\mathcal{T}_H^{\text{ren}} + 3\lambda\mathcal{T}_G^{\text{ren}} - 18\lambda^2\phi^2\mathcal{I}_{HH}^{\text{ren}}(p) - 6\lambda^2\phi^2\mathcal{I}_{GG}^{\text{ren}}(p) + \Pi_H^{2\text{PI},(2)}(p; \phi), \quad (\text{A.1a})$$

$$\Delta^{-1,G}(p; \phi) = p^2 + \lambda\phi^2 - m^2 + \lambda\mathcal{T}_H^{\text{ren}} + 5\lambda\mathcal{T}_G^{\text{ren}} - 4\lambda^2\phi^2\mathcal{I}_{GH}^{\text{ren}}(p) + \Pi_G^{2\text{PI},(2)}(p; \phi), \quad (\text{A.1b})$$

$$\frac{1}{\phi} \frac{d\tilde{V}_{\text{eff}}(\phi)}{d\phi} = \Delta^{-1,G}(0; \phi), \quad (\text{A.1c})$$

where the $\overline{\text{MS}}$ renormalized sunset and tadpole integrals are given by [20]

$$\mathcal{I}_{ab}^{\text{ren}}(p) \equiv \int_k \left(\Delta^a(k-p) \Delta^b(k) - \frac{1}{(k^2 + \mu^2)^2} \right), \quad (\text{A.2})$$

$$\mathcal{T}_a^{\text{ren}} \equiv \int_k \left[\Delta^a(k) - \frac{1}{k^2 + \mu^2} - \frac{1}{(k^2 + \mu^2)^2} \left(\mu^2 - M_a^2 + \frac{\nu_a \lambda^2 \phi^2}{16\pi^2} B(p; \mu^2, \mu^2) \right) \right] - \frac{\mu^2}{16\pi^2} + \frac{\nu_a \lambda^2 \phi^2}{(16\pi^2)^2} \frac{\eta}{2}, \quad (\text{A.3})$$

where $\nu_H = 24$, $\nu_G = 4$ and we have introduced

$$\frac{1}{16\pi^2} B(p; \mu^2, \mu^2) \equiv \mathcal{I}_{00}^{\text{ren}}(p), \quad \text{with} \quad \Delta^0(k) \equiv \frac{1}{k^2 + \mu^2}, \quad (\text{A.4})$$

$$\eta = 1 - \frac{4i}{\sqrt{3}} \left(\text{Li}_2 \frac{1 - i\sqrt{3}}{2} - \frac{\pi^2}{36} \right) \simeq -1.34391. \quad (\text{A.5})$$

Here, we seize the opportunity to eliminate an error in the value of η reported in [20]. The terms in the second line of (A.3) are the $\overline{\text{MS}}$ finite part of the CT integrals used to renormalize \mathcal{T}_a by the method discussed in [20]. Their subtraction is needed to guarantee that the renormalization scheme used here matches the standard $\overline{\text{MS}}$ one in perturbation theory. Finally, the 2-loop 2PI self-energies $\Pi_{H,G}^{2\text{PI},(2)}(p; \phi)$ are calculated in perturbation theory by standard techniques [35, 36]. We approximate them by their zero-momentum value $\Pi_{H,G}^{2\text{PI},(2)}(\phi)$, since the error introduced in this way is expected to be negligible for the purposes of this work. Adopting the compact notation used in [35], in terms of the functions defined there we find

$$\begin{aligned} (16\pi^2)^2 \Pi_H^{2\text{PI},(2)}(\phi) &= 54\lambda^3 \phi^2 \overline{\ln}^2 H + 36\lambda^3 \phi^2 \overline{\ln} H \overline{\ln} G + 30\lambda^3 \phi^2 \overline{\ln}^2 G \\ &\quad - 6\lambda^2 I(H, H, H) - 6\lambda^2 I(H, G, G) \\ &\quad - 216\lambda^3 \phi^2 I(H', H, H) - 72\lambda^3 \phi^2 I(H', G, G) - 24\lambda^3 \phi^2 I(G', G, H) \\ &\quad - 648\lambda^4 \phi^4 I(H', H', H) - 144\lambda^4 \phi^4 I(H', G', G) - 24\lambda^4 \phi^4 I(G', G', H), \end{aligned} \quad (\text{A.6a})$$

$$\begin{aligned} (16\pi^2)^2 \Pi_G^{2\text{PI},(2)}(\phi) &= 8\lambda^3 \phi^2 B(G, H)^2 - 24\lambda^2 I(H, H, H) + 22\lambda^2 I(G, H, H) \\ &\quad - 16\lambda^2 I(G, G, H) + 6\lambda^2 I(G, G, G), \end{aligned} \quad (\text{A.6b})$$

where all functions have to be evaluated at zero momentum.

References

- [1] F. Bezrukov, M. Y. Kalmykov, B. A. Kniehl and M. Shaposhnikov, JHEP **1210** (2012) 140 [arXiv:1205.2893 [hep-ph]].
- [2] G. Degrassi, S. Di Vita, J. Elias-Miro, J. R. Espinosa, G. F. Giudice, G. Isidori and A. Strumia, JHEP **1208** (2012) 098 [arXiv:1205.6497 [hep-ph]].
- [3] D. Buttazzo, G. Degrassi, P. P. Giardino, G. F. Giudice, F. Sala, A. Salvio and A. Strumia, JHEP **1312** (2013) 089 [arXiv:1307.3536 [hep-ph]].
- [4] J. M. Cornwall, R. Jackiw, E. Tomboulis, Phys. Rev. **D10** (1974) 2428–2445.
- [5] J. P. Blaizot, E. Iancu and A. Rebhan, Phys. Rev. D **63** (2001) 065003 [hep-ph/0005003].
- [6] J. Berges, S. Borsanyi, U. Reinosa and J. Serreau, Phys. Rev. D **71** (2005) 105004 [hep-ph/0409123].
- [7] G. Markó, U. Reinosa and Z. Szép, Phys. Rev. D **87** (2013) 10, 105001 [arXiv:1303.0230 [hep-ph]].
- [8] M. G. Alford, S. K. Mallavarapu, A. Schmitt and S. Stetina, Phys. Rev. D **89** (2014) 8, 085005 [arXiv:1310.5953 [hep-ph]].
- [9] G. Fejos, Phys. Rev. D **90** (2014) 11, 116001 [arXiv:1410.1337 [hep-ph]].
- [10] J. Berges, AIP Conf. Proc. **739** (2005) 3 [hep-ph/0409233].
- [11] P. Millington and A. Pilaftsis, Phys. Rev. D **88** (2013) 8, 085009 [arXiv:1211.3152 [hep-ph]].
- [12] A. Meistrenko, C. Wesp, H. van Hees and C. Greiner, J. Phys. Conf. Ser. **503** (2014) 012003 [arXiv:1311.7444 [hep-ph]].
- [13] P. S. Bhupal Dev, P. Millington, A. Pilaftsis and D. Teresi, Nucl. Phys. B **891** (2015) 128 [arXiv:1410.6434 [hep-ph]].
- [14] J. Goldstone, Nuovo Cim. **19** (1961) 154–164.
- [15] J. Goldstone, A. Salam, S. Weinberg, Phys. Rev. **127** (1962) 965–970.
- [16] G. Baym, G. Grinstein, Phys. Rev. **D15** (1977) 2897–2912.
- [17] G. Amelino-Camelia, Phys. Lett. **B407** (1997) 268–274.
- [18] N. Petropoulos, J. Phys. **G25** (1999) 2225–2241.

- [19] J. T. Lenaghan, D. H. Rischke, *J. Phys.* **G26** (2000) 431–450.
- [20] A. Pilaftsis and D. Teresi, *Nucl. Phys. B* **874** (2013) 2, 594 [arXiv:1305.3221 [hep-ph]].
- [21] H. Mao, *Nucl. Phys. A* **925** (2014) 185 [arXiv:1305.4329 [hep-ph]].
- [22] M. J. Brown and I. B. Whittingham, arXiv:1502.03640 [hep-th].
- [23] S. P. Martin, *Phys. Rev. D* **89** (2014) 1, 013003 [arXiv:1310.7553 [hep-ph]].
- [24] S. P. Martin, *Phys. Rev. D* **90** (2014) 1, 016013 [arXiv:1406.2355 [hep-ph]].
- [25] J. Elias-Miro, J. R. Espinosa and T. Konstandin, *JHEP* **1408** (2014) 034 [arXiv:1406.2652 [hep-ph]].
- [26] A. Pilaftsis and D. Teresi, in preparation.
- [27] G. Baym, *Phys. Rev.* **127** (1962) 1391.
- [28] H. van Hees, J. Knoll, *Phys. Rev.* **D65** (2002) 025010.
- [29] J.-P. Blaizot, E. Iancu, U. Reinosa, *Nucl. Phys.* **A736** (2004) 149–200.
- [30] J. Berges, S. Borsanyi, U. Reinosa, J. Serreau, *Annals Phys.* **320** (2005) 344–398.
- [31] H. van Hees, J. Knoll, *Phys. Rev.* **D66** (2002) 025028.
- [32] Y. Ivanov, F. Riek, J. Knoll, *Phys. Rev.* **D71** (2005) 105016.
- [33] Y. Ivanov, F. Riek, H. van Hees, J. Knoll, *Phys. Rev.* **D72** (2005) 036008.
- [34] E. J. Weinberg, A.-Q. Wu, *Phys. Rev.* **D36** (1987) 2474.
- [35] S. P. Martin, *Phys. Rev. D* **70** (2004) 016005 [hep-ph/0312092].
- [36] S. P. Martin, *Phys. Rev. D* **68** (2003) 075002 [hep-ph/0307101].